

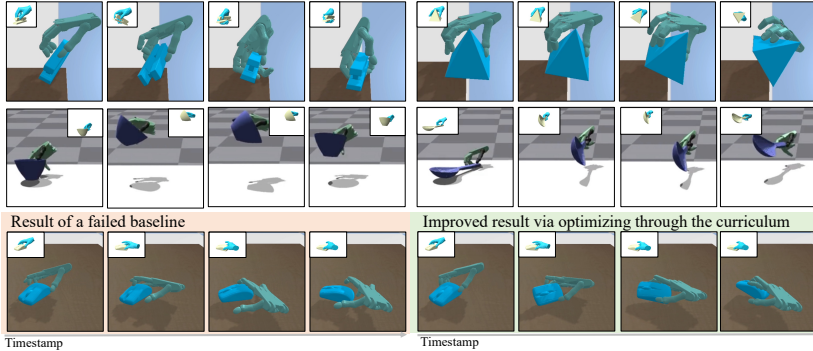
001

# Parameterized Quasi-Physical Simulators for 002 Dexterous Manipulations Transfer

003

003 Anonymous ECCV 2024 Submission

004 Paper ID #10032



005 **Fig. 1:** By optimizing through a **quasi-physical simulator curriculum**, we successfully  
006 transfer human demonstrations to dexterous robot hand simulations. We enable  
007 accurate tracking of complex manipulations with changing contacts (*Fig. (a)*), non-  
008 trivial object motions (*Fig. (b)*) and intricate tool-using (*Fig. (c,d)*). Besides, our  
009 physics curriculum can substantially improve the performance of a failed baseline as  
010 well (*Fig. (e,f)*).  
011

012 **Abstract.** We explore the dexterous manipulation transfer problem by  
013 designing simulators. The task wishes to transfer human manipulations  
014 to dexterous robot hand simulations and is inherently difficult due to  
015 its intricate, highly-constrained, and discontinuous dynamics and the  
016 need to control a dexterous hand with a DoF to accurately replicate hu-  
017 man manipulations. Previous approaches that optimize in high-fidelity  
018 black-box simulators or a modified one with relaxed constraints only  
019 demonstrate limited capabilities or are restricted by insufficient simula-  
020 tion fidelity. We introduce **parameterized quasi-physical simulators**  
021 and a **physics curriculum** to overcome these limitations. The key ideas  
022 are 1) balancing between fidelity and optimizability of the simulation via  
023 a curriculum of parameterized simulators, and 2) solving the problem in  
024 each of the simulators from the curriculum, with properties ranging from  
025 high task optimizability to high fidelity. We successfully enable a dex-  
026 terous hand to track complex and diverse manipulations in high-fidelity  
027 simulated environments, boosting the success rate by 11%+ from the  
028 best-performed baseline. We include a [website](#) to introduce the work.  
029

030 **Keywords:** Dexterous Manipulation Transfer · Hybrid Simulation

023

# 1 Introduction

Advancing an embodied agent’s capacity to interact with the world represents a significant stride toward achieving general artificial intelligence. Due to the substantial costs and potential hazards of setting up real robots to do trial and error, the standard approach for developing embodied algorithms involves learning in physical simulators [9, 15, 23, 25, 33, 56, 59] before transitioning to real-world deployment. In most cases, physical simulators are treated as black boxes, and extensive efforts have been devoted to developing learning and optimization methods for embodied skills within these black boxes. Despite the considerable progress [2, 6–8, 16, 20, 21, 31, 36, 39, 43, 46, 60, 62, 66, 68], the question like whether the simulators used are the most suitable ones is rarely discussed. In this work, we investigate this issue and illustrate how optimizing the simulator concurrently with skill acquisition can benefit a popular yet challenging task in robot manipulation – dexterous manipulation transfer.

The task aims at transferring human-object manipulations to a dexterous robot hand, enabling it to physically track the reference motion of both the hand and the object (see Fig. 1). It is challenged by 1) the complex, highly constrained, non-smooth, and discontinuous dynamics with frequent contact establishment and breaking involved in the robot manipulation, 2) the requirement of precisely controlling a dexterous hand with a high DoF to densely track the manipulation at each frame, and 3) the morphology difference. Some existing works rely on high-fidelity black-box simulators, where a small difference in robot control can result in dramatically different manipulation outcomes due to abrupt contact changes, making the tracking objective highly non-smooth and hard to optimize [4, 6, 8, 43, 46]. In this way, their tasks are restricted to relatively simple goal-driven manipulations such as pouring and re-locating [8, 43, 46, 68], in-hand re-orientation, flipping and spinning [4, 6] with a fixed-root robot hand, or manipulating objects with simple geometry such as balls [36]. Other approaches attempt to improve optimization by relaxing physical constraints, with a primary focus on smoothing out contact responses [3, 24, 38, 55, 56]. However, their dynamics models may significantly deviate from real physics [38], hindering skill deployment. Consequently, we ask how to address the optimization challenge while preserving the high fidelity of the simulator.

Our key insight is that a single simulator can hardly provide both high fidelity and excellent optimizability for contact-rich dexterous manipulations. Inspired by the line of homotopy methods [12, 28, 29, 61], we propose a curriculum of simulators to realize this. We start by utilizing a quasi-physical simulator to initially relax physical constraints and warm up the optimization. Subsequently, we transfer the optimization outcomes to simulators with gradually tightened physical constraints. Finally, we transition to a physically realistic simulator for skill deployment in realistic dynamics.

To realize this vision, we propose a **family of parameterized quasi-physical simulators** for contact-rich dexterous manipulation tasks. These simulators can be customized to enhance task optimizability while can also be tailored to approximate realistic physics. The parameterized simulator represents

023

024

025

026

027

028

029

030

031

032

033

034

035

036

037

038

039

040

041

042

043

044

045

046

047

048

049

050

051

052

053

054

055

056

057

058

059

060

061

062

063

064

065

066

067

an articulated multi rigid body as a parameterized point set, models contact using an unconstrained parameterized spring-damper, and compensates for unmodeled effects via parameterized residual physics. Specifically, the articulated multi-body dynamics model is relaxed as the point set dynamics model. An articulated object is relaxed into a set of points, sampled from the ambient space surrounding each body’s surface mesh. The resulting dynamics model combines the original articulated dynamics with the mass-point dynamics of each individual point. Parameters are introduced to control the point set construction and the dynamics model. The contact model is softened as a parameterized spring-damper model [3, 19, 35, 38, 51] with parameters introduced to control when to calculate contacts and contact spring stiffness. The residual physics network compensate for unmodeled effects from the analytical modeling [22]. The parameterized simulator can be programmed for high optimizability by relaxing constraints in the analytical model and can be tailored to approximate realistic physics by learning excellent residual physics. We demonstrate that the challenging dexterous manipulation transfer task can be effectively addressed through curriculum optimization using a series of parameterized physical simulators. Initially, both articulated rigid constraints and the contact model stiffness are relaxed in the simulator. It may not reflect physical realism but provides a good environment where the manipulation transfer problem can be solved easily. Subsequently, the articulated rigid constraints and the contact model are gradually tightened. Task-solving proceeds iteratively within each simulator in the curriculum. Finally, the parameterized simulator is optimized to approximate realistic physics. Task optimization continues, yielding a dexterous hand trajectory capable of executing the manipulation in environments with realistic physics.

We demonstrate the superiority of our method and compare it with previous model-free and model-based methods on challenging manipulation sequences from three datasets, describing single-hand or bimanual manipulations with daily objects or using tools. We conduct dexterous manipulation transfer on two widely used simulators, namely Bullet [9] and Isaac Gym [33] to demonstrate the generality and the efficacy of our method and the capability of our quasi-physical simulator to approximate the unknown black-box physics model in the contact-rich manipulation scenario (Fig. 1). We can track complex manipulations involving non-trivial object motions such as large rotations and complicated tool-using such as using a spoon to bring the water back and forth. Our approach successfully surpasses the previous best-performed method both quantitatively and qualitatively, achieving more than 11% success rate than the previous best-performed method. Besides, optimizing through the physics curriculum can significantly enhance the performance of previously under-performed RL-based methods, almost completing the tracking problem from failure, as demonstrated in Fig. 1. This indicates the universality of our approach to embodied AI through optimization via a physics curriculum. Thorough ablations are conducted to validate the efficacy of our designs.

Our contributions are three-fold:

- 113 – We introduce a family of parameterized quasi-physical simulators that can  
114 be configured to relax various physical constraints, facilitating skill optimiza-  
115 tion, and can also be tailored to achieve high simulation fidelity.
- 116 – We present a quasi-physics curriculum along with a corresponding optimi-  
117 zation method to address the challenging dexterous manipulation transfer  
118 problem.
- 119 – Extensive experiments demonstrate the effectiveness of our method in trans-  
120 ferring complex manipulations, including non-trivial object motions and  
121 changing contacts, to a dexterous robot hand in simulation.

## 122 2 Related Works

123 **Dexterous manipulation transfer.** Transferring human manipulations to  
124 dexterous robot-hand simulations is an important topic in robot skill acquisi-  
125 tion [8, 21, 31, 43, 60, 62, 68, 70]. Most approaches treat the simulator as black-box  
126 physics models and try to learn skills directly from that [4, 6, 8, 43, 46]. However,  
127 their demonstrated capabilities are restricted to relatively simple tasks. Another  
128 trend of work tries to relax the physics model [37, 38] to create a better environ-  
129 ment for task optimization. However, due to the disparity between their mod-  
130eling approach and realistic physics, successful trials are typically demonstrated  
131 only in their simulators, which can hardly complete the task under physically  
132 realistic dynamics. In this work, we introduce various parameterized analytical  
133 relaxations to improve the task optimizability while compensating for unmodeled  
134 effects via residual physics networks so the fidelity would not be sacrificed.

135 **Learning for simulation.** Analytical methods can hardly approximate an ex-  
136 tremely realistic physical world despite lots of smart and tremendous efforts  
137 made in developing numerical algorithms [19, 23, 26, 27]. Recently, data-driven  
138 approaches have attracted lots of interest for their high efficiency and strong  
139 approximation ability [10, 11, 22, 40, 41, 50, 63]. Special network designs are pro-  
140 posed to learn the contact behaviour [22, 41]. We in this work propose to leverage  
141 an analytical-neural hybrid approach and carefully design network modules for  
142 approximating residual contact forces in the contact-rich manipulation scenario.

143 **Sim-to-Sim and Sim-to-Real transfer.** The field of robot manipulation con-  
144 tinues to face challenges in the areas of Sim2Sim and Sim2Real transferabil-  
145 ity [71]. Considering the modeling gaps, the optimal strategy learned in a specific  
146 simulator is difficult to transfer to a different simulator or the real world. There-  
147 fore, many techniques for solving the problem have been proposed, including  
148 imitation learning [34, 42, 43, 45, 46, 48], transfer learning [72], distillation [47, 57],  
149 residual physics [17, 67], and efforts on bridging the gap from the dynamics model  
150 aspect [22, 69]. Our parameterized simulators learn residual physics involved in  
151 contact-rich robot manipulations. By combining an analytical base with residual  
152 networks, we showcase their ability to approximate realistic physics.

## 153 3 Method

154 Given a human manipulation demonstration, composed of a human hand mesh  
155 trajectory and an object pose trajectory  $\{\mathcal{H}, \mathcal{O}\}$ , the goal is transferring the

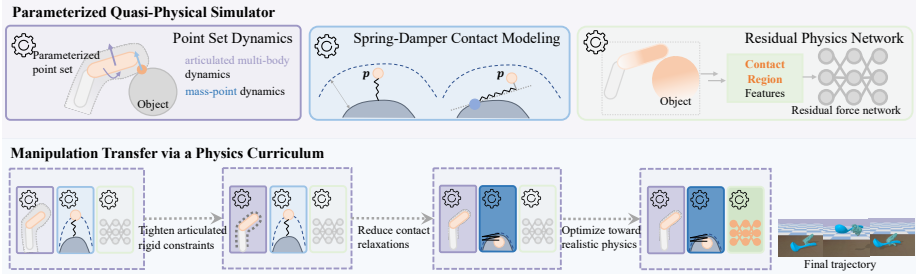


**Fig. 2:** The parameterized quasi-physical simulator relaxes the articulated multi rigid body dynamics as the *parameterized point set dynamics*, controls the contact behavior via an unconstrained *parameterized spring-damper contact model*, and compensates for unmodeled effects via *parameterized residual physics networks*. We tackle the difficult dexterous manipulation transfer problem via a **physics curriculum**.

demonstration to a dexterous robot hand in simulation. Formally, we aim to optimize a control trajectory  $\mathcal{A}$  that drives the dexterous hand to manipulate the object in a realistic simulated environment so that the resulting hand trajectory  $\hat{\mathcal{H}}$  and the object trajectory  $\hat{\mathcal{O}}$  are close to the reference motion  $\{\mathcal{H}, \mathcal{O}\}$ . The problem is challenged by difficulties from the highly constrained, discontinuous, and non-smooth dynamics, the requirement of controlling a high DoF dexterous hand for tracking, and the morphology difference.

Our method comprises two key designs to tackle the challenges: 1) a family of parameterized quasi-physical simulators, which can be programmed to enhance the optimizability of contact-rich dexterous manipulation tasks and can also be tailored to approximate realistic physics (Section 3.1), and 2) a physics curriculum that carefully adjusts the parameters of a line of quasi-physical simulators and a strategy that solves the difficult dexterous manipulation transfer task by addressing it within each simulator in the curriculum (Section 3.2).

### 3.1 Parameterized Quasi-Physical Simulators

Our quasi-physical simulator represents an articulated multi-body, *i.e.*, the robotic dexterous hand, as a point set. The object is represented as a signed distance field. The base of the simulator is in an analytical form leveraging an unconstrained spring-damper contact model. Parameters are introduced to control the analytical relaxations on the articulated rigid constraints and the softness of the contact model. Additionally, neural networks are introduced to compensate for unmodeled effects beyond the analytical framework. We will elaborate on each of these design aspects below.

**Parameterized point set dynamics.** Articulated multi-body represented in the reduced coordinate system [19, 59] may require a large change in joint states to achieve a small adjustment in the Euclidean space. Moving the end effector from one point to a nearby point may require adjusting all joint states (Fig. 3). Besides, transferring the hand trajectory to a morphologically different hand requires correspondences to make the resulting trajectory close to the original one. Defining correspondences in the reduced coordinate or via sparse correspon-

dences will make the result suffer from noise in the data, leading to unwanted results finally (Fig. 3). Hence, we propose relaxing an articulated multi-rigid body into a mass-point set sampled from the ambient space surrounding each body. Each point is considered attached to the body from which it is sampled and is capable of both self-actuation and actuation via joint motors. We introduce a parameter  $\alpha$  to control the point set construction and the dynamics. This representation allows an articulated rigid object to behave similarly to a deformable object, providing a larger action space to adjust its state and thereby easing the control optimization problem.

Specifically, for each body of the articulated object, we sample a set of points from the ambient space near the body mesh. The point set  $\mathcal{Q}$  is constructed by concatenating all sampled points together. Each point  $\mathbf{p}_i \in \mathcal{Q}$  is treated as a mass point with a finite mass  $\mathbf{m}_i$  and infinitesimal volume. The dynamics of the point set consist of articulated multi-body dynamics [14, 30], as well as the mass point dynamics of each point  $\mathbf{p}_i$ . For each  $\mathbf{p}_i$ , we have:

$$m_i \ddot{\mathbf{x}}_i = \mathbf{J}_i \mathbf{u} + \alpha \mathbf{f}_i + \alpha \mathbf{a}_i, \quad (1)$$

where  $\mathbf{J}_i$  represents the Jacobian mapping from the generalized velocity to the point velocity  $\dot{\mathbf{x}}_i$ ,  $\mathbf{u}$  denotes the generalized joint force,  $\mathbf{f}_i$  accounts for external forces acting on  $\mathbf{p}_i$ , and  $\mathbf{a}_i \in \mathbb{R}^3$  represents the actuation force applied to the point  $\mathbf{p}_i$ . Consequently, the point set is controlled by a shared control in the reduced coordinate space  $\mathbf{u}$  and per-point actuation force  $\mathbf{a}_i$ .

**Parameterized spring-damper contact modeling.** To ease the optimization challenges posed by contact-rich manipulations, which arise from contact constraints such as the non-penetration requirement and Coulomb friction law [3, 5], as well as discontinuous dynamics involving frequent contact establishment and breaking, we propose a parameterized contact model for relaxing constraints and controlling the contact behavior. Specifically, we leverage a classical unconstrained spring-damper model [19, 35, 51, 59, 64] to model the contacts. This model allows us to flexibly adjust the contact behavior by tuning the contact threshold and the spring stiffness coefficients. Intuitively, a contact model with a high threshold and low spring stiffness presents “soft” behaviors, resulting in a continuous and smooth optimization space. This makes optimization through such a contact model relatively easy. Conversely, a model with a low threshold and large stiffness coefficients will produce “stiff” behaviors, increasing the discontinuity of the optimization space due to frequent contact establishment and breaking. However, it also becomes more physically realistic, meaning contact forces are calculated only when two objects collide, and a large force is applied to separate them if penetrations are observed, thus better satisfying the non-penetration condition. Therefore, by adjusting the contact distance threshold

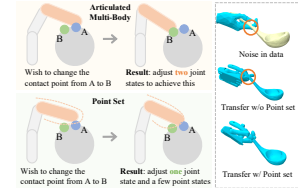


**Fig. 3: Point Set** can flexibly adjust its states, avoid overfitting to data noise, and ease the difficulty brought by the morphology difference.

and spring stiffness coefficients, we can modulate the optimizability and fidelity of the contact model. The parameter set of the contact model comprises a distance threshold  $d^c$  and spring stiffness coefficients. Next, we will delve into the details of the contact establishment, breaking, and force calculations processes.

Contacts are established between points in the manipulator's point set  $\mathcal{Q}$  and the object. A point  $\mathbf{p} \in \mathcal{Q}$  is considered to be in "contact" with the object if its signed distance to the object  $sd(\mathbf{p})$  is smaller than the contact distance threshold  $d^c$ . Subsequently, the object surface point nearest to  $\mathbf{p}$  is identified as the corresponding contact point on the object, denoted as  $\mathbf{p}^o$ . The normal direction of the object point  $\mathbf{p}^o$  is then determined as the contact normal direction, denoted as  $\mathbf{n}^o$ . The contact force  $\mathbf{f}^c$  applied from the manipulator point  $\mathbf{p}$  to  $\mathbf{p}^o$  is calculated as follows:

$$\mathbf{f}^c = -(k^n d - k^d d\dot{d})\mathbf{n}^o, \quad (2)$$

where,  $k^n$  represents the spring stiffness coefficient,  $k^d$  denotes the damping coefficient, and  $d = d^c - sd(\mathbf{p})$  is always positive. To enhance the continuity of  $\mathbf{f}^c$  [64],  $k^d d\dot{d}$  is used as the magnitude of the damping force, rather than  $k^d \dot{d}$ .

Friction forces are modeled as penalty-based spring forces [3, 65]. Once a point  $\mathbf{p}$  is identified as in contact with the object, with the object contact point denoted as  $\mathbf{p}^o$ , the contact pair is stored. Contact forces between them are continually calculated until the contact breaking conditions are met. In more detail, the static friction force from  $\mathbf{p}$  to  $\mathbf{p}^o$  is calculated using a spring model:

$$\mathbf{f}_s^f = k^f \mathbf{T}_n(\mathbf{p} - \mathbf{p}^o), \quad (3)$$

where  $k^f$  is the friction spring stiffness coefficient,  $\mathbf{T}_n = \mathbf{I} - \mathbf{n}^o \mathbf{n}^{oT}$  is a tangential projection operator. When the static friction satisfies  $\|\mathbf{f}_s^f\| \leq \mu \|\mathbf{f}^c\|$ ,  $\mathbf{f}_s^f$  is applied to the object point  $\mathbf{p}^o$ . Otherwise, the dynamic friction force is applied, and the contact breaks:

$$\mathbf{f}_d^f = -\mu \|\mathbf{f}_s^f\| \frac{\mathbf{T}_n \mathbf{v}_{\mathbf{p} \leftarrow \mathbf{p}^o}}{\|\mathbf{T}_n \mathbf{v}_{\mathbf{p} \leftarrow \mathbf{p}^o}\|}, \quad (4)$$

where  $\mathbf{v}_{\mathbf{p} \leftarrow \mathbf{p}^o}$  is the relative velocity between  $\mathbf{p}$  and  $\mathbf{p}^o$ .

**Parameterized residual physics.** The analytical designs facilitate relaxation but may limit the use of highly sophisticated and realistic dynamics models, deviating from real physics. To address this, the final component of our quasi-physical simulator is a flexible neural residual physics model [1, 22, 41].

Specifically, we propose to use networks to learn to predict residual contact forces and friction forces from contact-related information. For fine-grained residual contact force prediction, we design a local contact network  $f_{\psi_{\text{local}}}$  that inherits contact information identified in the parameterized contact model and predicts residual forces between each contact pair. To close the gap caused by contact region identification between the parameterized contact model and real contact region, we further include a global residual network  $f_{\psi_{\text{global}}}$  that predicts residual forces and torques added directly to the object's center of mass. In more detail, given a contact pair  $(\mathbf{p}, \mathbf{p}^o)$ , the local contact network maps the contact-related features of the local contact region, consisting of geometry, per-point velocity, and per object point normal, to the residual contact force and residual

friction force between such two points in the contact pair. The global residual network additionally takes contact-related information of the global contact region, including the geometry, per-point velocity, and per-object point normal, as input and predicts a residual force and residual torque added to the object’s center of mass. Details such as contact region identification and network architectures are deferred to the Supp. We denote the optimizable parameters in the residual physics network as  $\psi = (\psi_{\text{global}}, \psi_{\text{local}})$ . By optimizing the residual physics network, we unlock the possibility of introducing highly non-linear dynamics to align our parametrized quasi-physical simulator with any realistic black-box physical simulator.

Semi-implicit time-stepping is leveraged to make the simulation auto differentiable and easy to combine with neural networks [22].

### 3.2 Dexterous Manipulation Transfer via a Physics Curriculum

Based on the family of parameterized quasi-physical simulators, we propose to solve the challenging dexterous manipulation transfer problem via a physics curriculum. It is constructed by a series of parameterized simulators varying from the one with few constraints and the softest contact behavior, gradually to a realistic simulator. We then solve the problem by transferring the demonstration to the dexterous hand in each simulator across the curriculum gradually. In more detail, the optimization starts from the parameterized simulator with both the articulated rigid constraints removed and the contact model tuned to the softest level. The residual physics networks are deactivated. It provides a friendly environment for optimization, and we can easily arrive at a workable hand trajectory here. Then the physics is gradually tightened and we solve the task in each simulator. After reaching the most tightened analytical model, the analytical part is fixed and residual networks are activated. The simulator is gradually optimized to approximate the dynamics in a realistic physical environment. At the same time, the control trajectory  $\mathcal{A}$  continues to be refined in the quasi-physical simulator. Finally, we arrive at a simulator optimized to be with high fidelity and a trajectory  $\mathcal{A}$  that can drive the dexterous hand to physically track the demonstration in a realistic simulated physical environment. Additionally, since object properties as well as system parameters like linear and angular velocity damping coefficients are unknown from the kinematics-only demonstration, we set them optimizable and identify them (denoted  $\mathcal{S}$ ) together with optimizing the hand control trajectory. Next we’ll illustrate this in detail.

**Transferring human demonstration via point set dynamics.** To robustly transfer the human demonstration to a morphologically different dexterous robot hand in simulation and to overcome noise in the kinematic trajectory, we initially relax the articulated rigid constraints and transfer the kinematics human demonstration to the control trajectory of the point set. Specifically, the point set representation with the relaxation parameter  $\alpha$  for the dynamic human hand [8] is constructed. The shared control trajectory  $\mathcal{A}$  and per-point per-frame actions are optimized so that the resulting trajectory of the point set can manipulate the object according to the demonstration. After that, a point set with the same

parameter  $\alpha$  is constructed to represent the dexterous robot hand. Subsequently, the shared control trajectory  $\mathcal{A}$  and per-point per-frame actions are optimized to track the manipulation accordingly.

**Transferring through a contact model curriculum.** After that, the articulated rigid constraint is tightened by freezing the point set parameter  $\alpha$  to zero. The following optimization starts from a parameterized simulator with the softest contact model. We then gradually tighten the contact model by adjusting its distance threshold, contact force spring stiffness, etc. By curriculum optimizing the trajectory  $\mathcal{A}$  and parameters  $\mathcal{S}$  in each of the quasi-physical simulators, we finally arrive at the control trajectory that can drive a dexterous hand to accomplish the tracking task in the parameterized simulator with the most tightened analytical model.

**Optimizing towards a realistic physical environment.** Subsequently, the residual physics network is activated and the parameterized simulator is optimized to approximate the dynamics in a realistic physical environment. We continue to optimize the hand trajectory in the quasi-physical simulator. Specifically, we leverage the successful trial in model-based human tracking literature [16, 66] and iteratively optimize the control trajectory  $\mathcal{A}$  and the parameterized simulator. In more detail, the following two subproblems are iteratively solved: 1) optimizing the quasi-physical simulator to approximate the realistic dynamics, and 2) optimizing the control trajectory  $\mathcal{A}$  to complete the manipulation in the quasi-physical simulator. Gradient-based optimization is leveraged taking advantage of the differentiability of the parameterized simulator.

After completing the optimization, the final control trajectory is yielded by model predictive control (MPC) [18] based on the optimized parameterized simulator and the hand trajectory  $\mathcal{A}$ . Specifically, in each step, the current and the following controls in several subsequent frames are optimized to reduce the tracking error. More details are deferred to the Supp.

## 4 Experiments

We conduct extensive experiments to demonstrate the effectiveness of our method. The evaluation dataset is constructed from three HOI datasets with both single-hand and bimanual manipulations (with rigid objects), with complex manipulations with non-trivial object movements, and rich and changing contacts involved (see Section 4.1). We use Shadow hand [49] and test in two simulators widely used in the embodied AI community: Bullet [9] and Isaac Gym [33]. We compare our method with both model-free approaches and model-based strategies and demonstrate the superiority of our method both quantitatively and qualitatively. We can track complex contact-rich manipulations with large object rotations, back-and-forth object movements, and changing contacts successfully in both of the two simulators, while the best-performed baseline fails (see Section 4.2, Fig. 4). On average, we boost the tracking success rate by 11%+ from the previous best-performed (see Section 4.2). We make further analysis and discussions and show that the core philosophy of our work, optimizing through a quasi-physics curriculum, is potentially general and can help improve the performance of a model-free baseline (see Section 4.3).

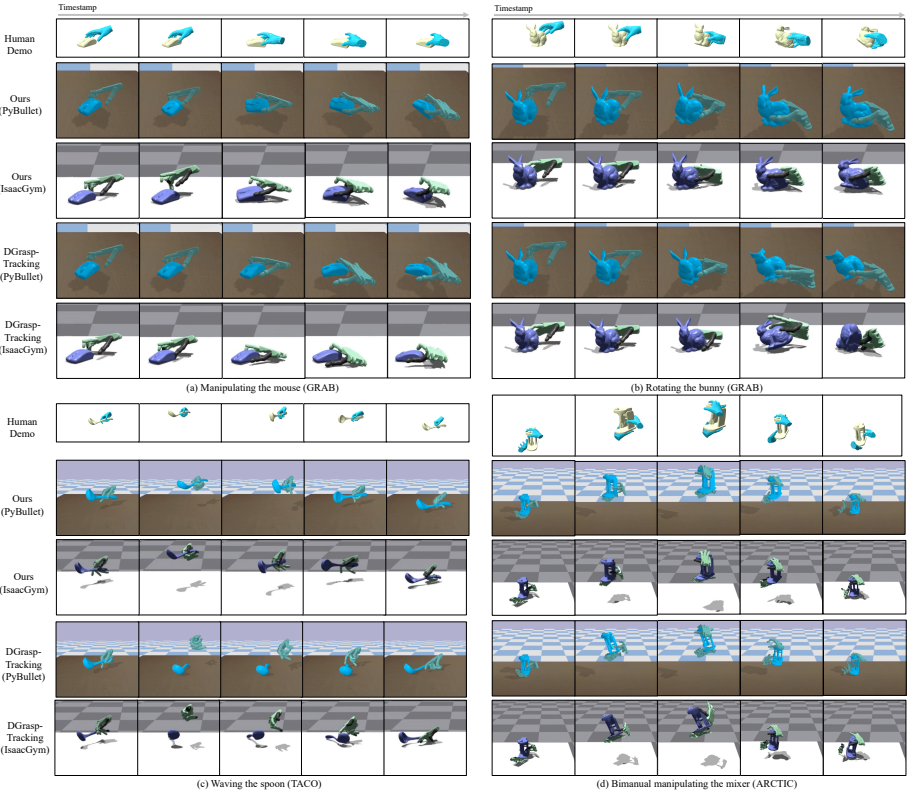


**Fig. 4: Qualitative comparisons.** Please refer to [our website](#) and the [supplementary video](#) for animated results.

## 362 4.1 Experimental Settings

**363 Datasets.** Our evaluation dataset is compiled from three distinct sources, namely  
**364** GRAB [53], containing single-hand interactions with daily objects, TACO [32],  
**365** containing humans manipulating tools, and ARCTIC [13] with bimanual manipulations.  
**366** For GRAB, we randomly sample a manipulation trajectory for each  
**367** object. If its manipulation is extremely simple, we additionally sample one tra-  
**368** jectory for it. The object is not considered if its corresponding manipulation  
**369** is bimanual such as `binoculars`, involves other body parts such as `bowl`, or  
**370** with detailed part movements such as the `game controller`. The number of  
**371** manipulation sequences from GRAB is 27. For TACO [32], we acquire data by  
**372** contacting authors. We randomly select one sequence for each right-hand tool ob-  
**373** ject. Sequences with very low quality like erroneous object motions are excluded.  
**374** 14 trajectories in total are selected finally. For ARCTIC [13], we randomly se-  
**375** lect one sequence for each object from its available manipulation trajectories,  
**376** resulting in 10 sequences in total. More details are deferred to the Supp.  
**377** **Metrics.** We introduce three distinct metrics to assess the quality of object  
**378** tracking, the accuracy of hand tracking, and the overall success of the tracking  
**379** task: 1) Per-frame average object rotation error:  $R_{\text{err}} = \frac{1}{N} \sum_{n=1}^N (1 - (\mathbf{q}_n \cdot \hat{\mathbf{q}}_n))$ ,

362  
363  
364  
365  
366  
367  
368  
369  
370  
371  
372  
373  
374  
375  
376  
377  
378  
379

380 where  $\mathbf{q}_n$  is the ground-truth orientation and  $\hat{\mathbf{q}}_n$  is the tracked result, represented in quaternion. 2) Per-frame average object translation error:  $T_{\text{err}} = \frac{1}{N} \sum_{n=1}^N \|\mathbf{t}_n - \hat{\mathbf{t}}_n\|$ , where  $\mathbf{t}$  and  $\mathbf{t}_n$  are ground-truth and tracked translations respectively. 3) Mean Per-Joint Position Error (MPJPE) =  $\frac{1}{N} \sum_{n=1}^N \|\mathbf{J}_n - \hat{\mathbf{J}}_n\|$  [20, 381 44, 58], where  $\mathbf{J}_n$  and  $\hat{\mathbf{J}}_n$  are keypoints of GT human hand and the simulated 382 robot hand respectively. We manually define the keypoints and the correspondences 383 to the human hand keypoints for the Shadow hand. 4) Per-frame average 384 hand Chamfer Distance:  $CD = \frac{1}{N} \sum_{n=1}^N \text{Chamfer-Distance}(\mathbf{H}_n - \hat{\mathbf{H}}_n)$ , for 385 evaluating whether the Shadow hand can “densely” track the demonstration. 386 5) Success rate: a tracking is regarded as successful if the object rotation 387 error  $R_{\text{err}}$ , object translation error  $T_{\text{err}}$ , and the hand tracking error MPJPE are 388 smaller than their corresponding threshold. Three success rates are calculated 389 using three different thresholds, namely  $10^\circ - 10\text{cm} - 10\text{cm}$ ,  $15^\circ - 15\text{cm} - 15\text{cm}$ . 390

391 **Baselines.** We compare with two trends of baselines. For model-free approaches, 392 since there is no prior work with exactly the same problem setting as us, we try to 393 modify and improve a goal-driven rigid object manipulation method DGrasp [8] 394 into two methods for tracking: 1) DGrasp-Base, where the method is almost kept 395 with same with the original DGrasp. We use the first frame where the hand and 396 the object are in contact with each other as the reference frame. Then the policy 397 is trained to grasp the object according to the reference hand and object goal 398 at first. After that, only the root is guided to complete the task. 2) DGrasp- 399 Tracking, where we divide the whole sequence into several subsequences, each of 400 which has 10 frames, and define the end frame of the subsequence as the reference 401 frame. Then the grasping policy is used to guide the hand and gradually track 402 the object according to the hand and the object pose of each reference frame. 403 We improve the DGrasp-Tracking by optimizing the policy through the quasi- 404 physical curriculum and creating “DGrasp-Tracking (w/ Curriculum)” trying to 405 improve its performance. For model-based methods, we compare with Control- 406 VAE [66] and traditional MPC approaches. For Control-VAE, we modify its 407 implementation for the manipulation tracking task. We additionally consider 408 three differentiable physics models to conduct model-predictive control for solving 409 the task. Taking the analytical model with the most tightened contact model 410 as the base model (“MPC (w/ base sim.”), we further augment it with a general 411 state-of-the-art contact smoothing for robot manipulation [52] and create “MPC 412 (w/ base sim. w/ soften)”. Details of baseline models are deferred to the Supp. 413

414 **Training and evaluation settings.** The physics curriculum is composed of 415 three stages. In the first stage, the parameter  $\alpha$  varies from 0.1 to 0.0 and the 416 contact model stiffness is relaxed to the softest level. In the second stage,  $\alpha$  is 417 fixed and the contact model stiffness varies from the softest version to the most 418 tightened level gradually through eight stages. Details w.r.t. parameter settings 419 are deferred to the Supp. In the first two stages, we alternately optimize the 420 trajectory  $\mathcal{A}$  and parameters  $\mathcal{S}$ . In each optimization iteration, the  $\mathcal{A}$  is optimized 421 for 100 steps while  $\mathcal{S}$  is optimized for 1000 steps. In the third stage,  $\mathcal{A}$  and  $\psi$  are 422 optimized for 256 steps in each iteration. For time-stepping,  $dt$  is set to  $5 \times 10^{-4}$  423 in the parameterized and the target simulators. The articulated multi-body is 424

**Table 1: Quantitative evaluations and comparisons to baselines.** **Bold red** numbers for best values and *italic blue* values for the second best-performed ones.

Simulator	Method	$R_{\text{err}}$ ( $^{\circ}, \downarrow$ )	$T_{\text{err}}$ ( $\text{cm}, \downarrow$ )	MPJPE ( $\text{mm}, \downarrow$ )	CD ( $\text{mm}, \downarrow$ )	Success Rate (% , $\uparrow$ )
Bullet	Model	DGrasp-Base	44.24	5.82	40.55	16.37
	Model	DGrasp-Tracking	44.45	5.04	37.56	14.72
	Free	DGrasp-Tracking (w/ curric.)	33.86	4.60	30.47	13.53
	Model	Control-VAE	42.45	<i>2.79</i>	25.21	10.94
	Based	MPC (w/ base sim.)	32.56	3.67	<i>24.62</i>	<i>10.80</i>
	Based	MPC (w/ base sim. w/ soften)	<i>31.89</i>	3.63	28.26	11.31
	Ours		<b>24.21</b>	<b>1.97</b>	<b>24.40</b>	<b>9.85</b>
	<b>Ours</b>		<b>25.97</b>	<b>2.08</b>	25.33	<b>10.31</b>
						<b>21.57/43.14/56.86</b>
Isaac Gym	Model	DGrasp-Base	36.41	4.56	50.97	18.78
	Model	DGrasp-Tracking	44.71	5.57	41.53	16.72
	Free	DGrasp-Tracking (w/ curric.)	38.75	5.13	40.09	16.26
	Model	Control-VAE	<i>35.40</i>	4.61	27.63	13.17
	Based	MPC (w/ base sim.)	37.23	4.73	<i>23.19</i>	<i>9.75</i>
	Based	MPC (w/ base sim. w/ soften)	36.40	<i>4.46</i>	<i>23.27</i>	10.34
	Ours		<b>25.97</b>	<b>2.08</b>	25.33	<b>10.31</b>
	<b>Ours</b>					<b>21.57/43.14/56.86</b>

controlled by joint motors and root velocities in the parameterized quasi-physical simulator while PD control [54] is leveraged in the target simulators.

## 4.2 Dexterous Manipulating Tracking

We conducted thorough experiments in two widely used simulators [9, 33]. We treat them as realistic simulated physical environments with high fidelity and wish to track the manipulation in them. In summary, we can control a dexterous hand to complete a wide range of the manipulation tracking tasks with non-trivial object movements and changing contacts. As presented in Table 1, we can achieve significantly higher success rates calculated under three thresholds than the best-performed baseline in both tested simulators. Fig. 4 showcases qualitative examples and comparisons. Please refer to our website and supplementary video for animated results.

**Complex manipulations.** For examples shown in Fig. 4, we can complete the tracking task on examples with large object re-orientations and complicated tool-using (Fig. (a,b,c)). However, DGrasp-Tracking fails to establish sufficient contact for correctly manipulating the object. In more detail, in Fig. 4(b), the bunny gradually bounced out from its hand in Bullet, while our method does not suffer from this difficulty. In Fig. 4(c), the spoon can be successfully picked up and waved back-and-forth in our method, while DGrasp-Tracking loses the track right from the start.

**Bimanual manipulations.** We are also capable of tracking bimanual manipulations. As shown in the example in Fig. 4(d), where two hands collaborate to relocate the object, DGrasp-Tracking fails to accurately track the object, while our method significantly outperforms it.

## 4.3 Further Analysis and Discussions

**Could model-free methods benefit from the physics curriculum?** In addition to the demonstrated merits of our quasi-physical simulators, we further explore whether model-free strategies can benefit from them. We introduce the “DGrasp-Tracking (w/ Curriculum)” method and compare its performance with

**Table 2: Ablation studies.** **Bold red** numbers for best values and *italic blue* values for the second best-performed ones. The simulation environment is Bullet.

Method	$R_{\text{err}}$ ( $^{\circ}, \downarrow$ )	$T_{\text{err}}$ ( $cm, \downarrow$ )	MPJPE ( $mm, \downarrow$ )	CD ( $mm, \downarrow$ )	Success Rate (% , $\uparrow$ )
Ours w/o Analytical Sim.	44.27	4.39	29.84	12.91	0/13.73/25.49
Ours w/o Residual Physics	33.69	3.81	<i>26.57</i>	10.34	5.88/23.53/41.18
Ours w/o Local Force NN	35.98	2.90	32.87	12.44	0/19.61/35.29
Ours w/o Curriculum	42.40	4.87	32.61	13.37	0/17.64/29.41
Ours w/ Curriculum II	<i>29.58</i>	<i>2.33</i>	31.61	<i>10.29</i>	<i>11.76/27.45/50.98</i>
Ours	<b>24.21</b>	<b>1.97</b>	<b>24.40</b>	<b>9.85</b>	<b>27.45/37.25/58.82</b>

the original DGrasp-Tracking model. As shown in Table 1 and the visual comparisons in Fig. 6, the DGrasp-Tracking model indeed benefits from a well-designed physics curriculum. For example, as illustrated in Fig. 6, the curriculum can significantly improve its performance, enabling it to nearly complete challenging tracking tasks where the original version struggles.

## 5 Ablation Study

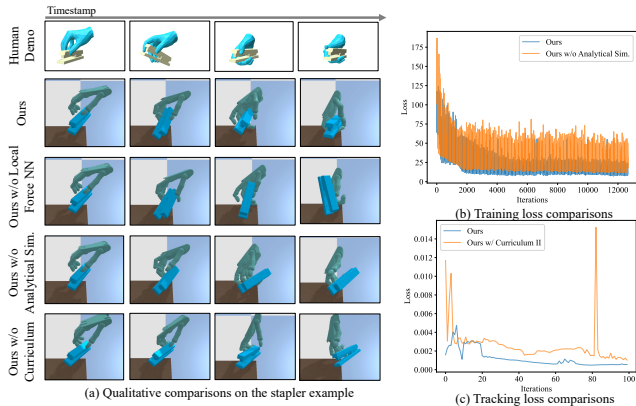


**Fig. 5:** (a) Qualitative comparisons between our full method and the ablated models; (b) Training loss curve comparisons; (c) Tracking loss curve comparisons.

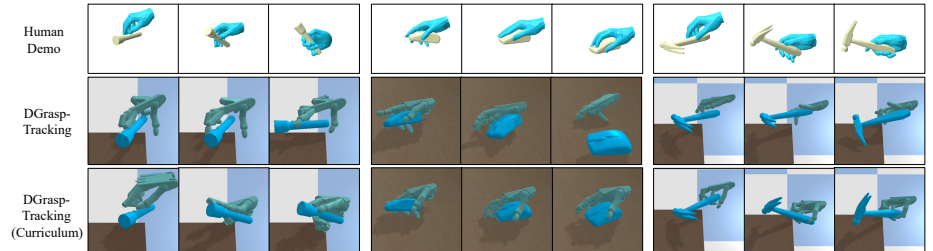


**Fig. 6:** Visual evidence on boosting DGrasp-Tracking’s performance via optimizing it through a physics curriculum.

We conduct a wide range of ablation studies to validate the effectiveness of some of our crucial designs, including the parameterized analytical physics model, the parameterized residual physics, the role of the local force network,

the necessity of introducing a physics curriculum into the optimization, and how the design on the curriculum stages affects the result.

**Parameterized analytical model.** The skeleton of the quasi-physical simulator is an analytical physics model. The intuition is that the parameterized simulator with such physical bias can be optimized towards a realistic simulator more easily than training pure neural networks for approximating. To validate this, we ablate the analytical model and use neural networks to approximate physics in Bullet directly (denoted as “Ours w/o Analytical Sim.”). The quantitative (Table 2) and qualitative (Fig. 5) results indicate that the physical biases brought by the analytical model could help the parameterized simulator to learn better physics in the contact-rich scenario. For instance, in the example demonstrated in Fig. 5, the ablated version fails to guide the robot hand to successfully pinch the object in the second figure.

**Parameterized residual physics.** To validate the necessity of introducing residual force networks to close the gap between the physics modeled in the parameterized analytical simulator and that of a realistic simulator, we ablate the parameterized force network and create a version named “Ours w/o Residual Physics”. Table 2 demonstrated its role in enabling the parameterized simulator to approximate realistic physics models.

**Local residual force network.** To adequately leverage state and contact-related information for predicting residual contact forces, we propose to use two types of networks: 1) a local force network for per contact pair residual forces and 2) a global network for additionally compensating. The local network is introduced for fine-grained approximation. We ablate this design and compare the result with our full model to validate this (see Fig. 5 and Table 1).

**Optimizing through an analytical physics curriculum.** We further investigate the effectiveness of the analytical curriculum design and how its design influences the result. Specifically, we create two ablated versions: 1) “Ours w/o Curriculum”, where the optimization starts directly from the parameterized analytical model with articulated rigid constraints tightened and the stiffest contact model, and 2) “Ours w/ Curriculum II”, where we move some stages out from the original curriculum. Table 2 and Fig. 5 demonstrate that both the curriculum and the optimization path will affect the model’s performance.

## 6 Conclusion and Limitations

In this work, we investigate creating better simulators for solving complex robotic tasks involving complicated dynamics where the previous best-performed optimization strategy fails. We present a family of parameterized quasi-physical simulators that can be both programmed to relax various constraints for task optimization and can be tailored to approximate realistic physics. We tackle the difficult manipulation transfer task via a physics curriculum.

**Limitations.** The method is limited by the relatively simple spring-damper model for contact constraint relaxation. Introducing delicate analytical contact models to parameterized simulators is an interesting research direction.

506

## References

- 507 1. Ajay, A., Wu, J., Fazeli, N., Bauza, M., Kaelbling, L.P., Tenenbaum, J.B., Rodriguez, A.: Augmenting physical simulators with stochastic neural networks: Case  
508 study of planar pushing and bouncing. In: 2018 IEEE/RSJ International Conference  
509 on Intelligent Robots and Systems (IROS). pp. 3066–3073. IEEE (2018) 7
- 510 2. Akkaya, I., Andrychowicz, M., Chociej, M., Litwin, M., McGrew, B., Petron, A.,  
511 Paino, A., Plappert, M., Powell, G., Ribas, R., et al.: Solving rubik’s cube with a  
512 robot hand. arXiv preprint arXiv:1910.07113 (2019) 2
- 513 3. Andrews, S., Erleben, K., Ferguson, Z.: Contact and friction simulation for  
514 computer graphics. In: ACM SIGGRAPH 2022 Courses, pp. 1–172 (2022) 2, 3, 6,  
515 7
- 516 4. Andrychowicz, O.M., Baker, B., Chociej, M., Jozefowicz, R., McGrew, B., Pachocki, J., Petron, A., Plappert, M., Powell, G., Ray, A., et al.: Learning dexterous  
517 in-hand manipulation. The International Journal of Robotics Research **39**(1), 3–20  
518 (2020) 2, 4
- 519 5. Baraff, D.: An introduction to physically based modeling: rigid body simulation  
520 ii—nonpenetration constraints. SIGGRAPH course notes pp. D31–D68 (1997) 6
- 521 6. Chen, T., Tippur, M., Wu, S., Kumar, V., Adelson, E., Agrawal, P.: Visual  
522 dexterity: In-hand reorientation of novel and complex object shapes. Science  
523 Robotics **8**(84), eadc9244 (2023). <https://doi.org/10.1126/scirobotics.adc9244>, <https://www.science.org/doi/abs/10.1126/scirobotics.adc9244> 2,  
524 4
- 525 7. Chen, T., Xu, J., Agrawal, P.: A system for general in-hand object re-orientation.  
526 Conference on Robot Learning (2021) 2
- 527 8. Christen, S., Kocabas, M., Aksan, E., Hwangbo, J., Song, J., Hilliges, O.: D-grasp:  
528 Physically plausible dynamic grasp synthesis for hand-object interactions. In: Pro-  
529 ceedings of the IEEE/CVF Conference on Computer Vision and Pattern Recog-  
530 nition. pp. 20577–20586 (2022) 2, 4, 8, 11
- 531 9. Coumans, E., Bai, Y.: Pybullet, a python module for physics simulation for games,  
532 robotics and machine learning (2016) 2, 3, 9, 12
- 533 10. Deng, Y., Yu, H.X., Wu, J., Zhu, B.: Learning vortex dynamics for fluid inference  
534 and prediction. arXiv preprint arXiv:2301.11494 (2023) 4
- 535 11. Du, T.: Deep learning for physics simulation. In: ACM SIGGRAPH 2023 Courses,  
536 pp. 1–25 (2023) 4
- 537 12. Dunlavy, D.M., O’Leary, D.P.: Homotopy optimization methods for global opti-  
538 mization. Tech. rep., Sandia National Laboratories (SNL), Albuquerque, NM, and  
539 Livermore, CA ... (2005) 2
- 540 13. Fan, Z., Taheri, O., Tzionas, D., Kocabas, M., Kaufmann, M., Black, M.J., Hilliges,  
541 O.: ARCTIC: A dataset for dexterous bimanual hand-object manipulation. In: Pro-  
542 ceedings IEEE Conference on Computer Vision and Pattern Recognition (CVPR)  
543 (2023) 10
- 544 14. Featherstone, R.: Rigid body dynamics algorithms (2007), <https://api.semanticscholar.org/CorpusID:58437819> 6
- 545 15. Freeman, C.D., Frey, E., Raichuk, A., Girgin, S., Mordatch, I., Bachem, O.: Brax—a  
546 differentiable physics engine for large scale rigid body simulation. arXiv preprint  
547 arXiv:2106.13281 (2021) 2
- 548 16. Fussell, L., Bergamin, K., Holden, D.: Supertrack: Motion tracking for physically  
549 simulated characters using supervised learning. ACM Transactions on Graphics  
550 (TOG) **40**(6), 1–13 (2021) 2, 9

507

508

509

510

511

512

513

514

515

516

517

518

519

520

521

522

523

524

525

526

527

528

529

530

531

532

533

534

535

536

537

538

539

540

541

542

543

544

545

546

547

548

549

550

551

552

553

554

- 555 17. Gao, J., Michelis, M.Y., Spielberg, A., Katzschmann, R.K.: Sim-to-real of soft  
556 robots with learned residual physics. arXiv preprint arXiv:2402.01086 (2024) 4  
557 18. Garcia, C.E., Prett, D.M., Morari, M.: Model predictive control: Theory and prac-  
558 tice—a survey. *Automatica* **25**(3), 335–348 (1989) 9  
559 19. Geilinger, M., Hahn, D., Zehnder, J., Bächer, M., Thomaszewski, B., Coros, S.:  
560 Add: Analytically differentiable dynamics for multi-body systems with frictional  
561 contact. *ACM Transactions on Graphics (TOG)* **39**(6), 1–15 (2020) 3, 4, 5, 6  
562 20. Grandia, R., Farshidian, F., Knoop, E., Schumacher, C., Hutter, M., Bächer, M.:  
563 Doc: Differentiable optimal control for retargeting motions onto legged robots.  
564 *ACM Transactions on Graphics (TOG)* **42**(4), 1–14 (2023) 2, 11  
565 21. Gupta, A., Eppner, C., Levine, S., Abbeel, P.: Learning dexterous manipulation for  
566 a soft robotic hand from human demonstrations. In: 2016 IEEE/RSJ International  
567 Conference on Intelligent Robots and Systems (IROS). pp. 3786–3793. IEEE (2016)  
568 2, 4  
569 22. Heiden, E., Millard, D., Coumans, E., Sheng, Y., Sukhatme, G.S.: Neuralsim:  
570 Augmenting differentiable simulators with neural networks. In: 2021 IEEE Inter-  
571 national Conference on Robotics and Automation (ICRA). pp. 9474–9481. IEEE  
572 (2021) 3, 4, 7, 8  
573 23. Howell, T.A., Le Cleac'h, S., Kolter, J.Z., Schwager, M., Manchester, Z.: Dojo: A  
574 differentiable simulator for robotics. arXiv preprint arXiv:2203.00806 9 (2022) 2,  
575 4  
576 24. Howell, T.A., Le Cleac'h, S., Singh, S., Florence, P., Manchester, Z., Sindhwan, V.: Trajectory optimization with optimization-based dynamics. *IEEE Robotics and  
577 Automation Letters* **7**(3), 6750–6757 (2022) 2  
578 25. Hwangbo, J., Lee, J., Hutter, M.: Per-contact iteration method for solving contact  
579 dynamics. *IEEE Robotics and Automation Letters* **3**(2), 895–902 (2018) 2  
580 26. Lan, L., Yang, Y., Kaufman, D., Yao, J., Li, M., Jiang, C.: Medial ipc: accelerated  
581 incremental potential contact with medial elastics. *ACM Transactions on Graphics*  
582 **40**(4) (2021) 4  
583 27. Li, M., Ferguson, Z., Schneider, T., Langlois, T.R., Zorin, D., Panozzo, D., Jiang,  
584 C., Kaufman, D.M.: Incremental potential contact: intersection-and inversion-free,  
585 large-deformation dynamics. *ACM Trans. Graph.* **39**(4), 49 (2020) 4  
586 28. Liao, S.: On the homotopy analysis method for nonlinear problems. *Applied math-  
587 ematics and computation* **147**(2), 499–513 (2004) 2  
588 29. Lin, X., Yang, Z., Zhang, X., Zhang, Q.: Continuation path learning for homotopy  
589 optimization (2023) 2  
590 30. Liu, C.K., Jain, S.: A quick tutorial on multibody dynamics. Online tutorial, June  
591 p. 7 (2012) 6  
592 31. Liu, X., Pathak, D., Kitani, K.M.: Herd: Continuous human-to-robot evolution for  
593 learning from human demonstration. arXiv preprint arXiv:2212.04359 (2022) 2, 4  
594 32. Liu, Y., Yang, H., Si, X., Liu, L., Li, Z., Zhang, Y., Liu, Y., Yi, L.: Taco: Bench-  
595 marking generalizable bimanual tool-action-object understanding. arXiv preprint  
596 arXiv:2401.08399 (2024) 10  
597 33. Makoviychuk, V., Wawrzyniak, L., Guo, Y., Lu, M., Storey, K., Macklin, M.,  
598 Hoeller, D., Rudin, N., Allshire, A., Handa, A., et al.: Isaac gym: High performance  
599 gpu-based physics simulation for robot learning. arXiv preprint arXiv:2108.10470  
600 (2021) 2, 3, 9, 12  
601 34. Mandikal, P., Grauman, K.: Dexvip: Learning dexterous grasping with human hand  
602 pose priors from video. In: Conference on Robot Learning. pp. 651–661. PMLR  
603 (2022) 4

- 605 35. Marcucci, T., Gabicci, M., Artoni, A.: A two-stage trajectory optimization strat-  
606 egy for articulated bodies with unscheduled contact sequences. *IEEE Robotics and  
607 Automation Letters* **2**(1), 104–111 (2016) [3](#), [6](#)
- 608 36. Mordatch, I., Popović, Z., Todorov, E.: Contact-invariant optimization for hand  
609 manipulation. In: Proceedings of the ACM SIGGRAPH/Eurographics symposium  
610 on computer animation. pp. 137–144 (2012) [2](#)
- 611 37. Pang, T., Suh, H.T., Yang, L., Tedrake, R.: Global planning for contact-rich manip-  
612 ulation via local smoothing of quasi-dynamic contact models. *IEEE Transactions  
613 on Robotics* (2023) [4](#)
- 614 38. Pang, T., Tedrake, R.: A convex quasistatic time-stepping scheme for rigid multi-  
615 body systems with contact and friction. In: 2021 IEEE International Conference  
616 on Robotics and Automation (ICRA). pp. 6614–6620. IEEE (2021) [2](#), [3](#), [4](#)
- 617 39. Peng, X.B., Abbeel, P., Levine, S., Van de Panne, M.: Deepmimic: Example-guided  
618 deep reinforcement learning of physics-based character skills. *ACM Transactions  
619 On Graphics (TOG)* **37**(4), 1–14 (2018) [2](#)
- 620 40. Pfaff, T., Fortunato, M., Sanchez-Gonzalez, A., Battaglia, P.W.: Learning mesh-  
621 based simulation with graph networks. *arXiv preprint arXiv:2010.03409* (2020) [4](#)
- 622 41. Pfrommer, S., Halm, M., Posa, M.: Contactnets: Learning discontinuous contact  
623 dynamics with smooth, implicit representations. In: Conference on Robot Learning.  
624 pp. 2279–2291. PMLR (2021) [4](#), [7](#)
- 625 42. Qin, Y., Su, H., Wang, X.: From one hand to multiple hands: Imitation learning  
626 for dexterous manipulation from single-camera teleoperation. *IEEE Robotics and  
627 Automation Letters* **7**(4), 10873–10881 (2022) [4](#)
- 628 43. Qin, Y., Wu, Y.H., Liu, S., Jiang, H., Yang, R., Fu, Y., Wang, X.: Dexmv: Imitation  
629 learning for dexterous manipulation from human videos. In: European Conference  
630 on Computer Vision. pp. 570–587. Springer (2022) [2](#), [4](#)
- 631 44. Qin, Y., Yang, W., Huang, B., Van Wyk, K., Su, H., Wang, X., Chao, Y.W., Fox, D.:  
632 Anyteleop: A general vision-based dexterous robot arm-hand teleoperation system.  
633 *arXiv preprint arXiv:2307.04577* (2023) [11](#)
- 634 45. Radosavovic, I., Wang, X., Pinto, L., Malik, J.: State-only imitation learning for  
635 dexterous manipulation. In: 2021 IEEE/RSJ International Conference on Intelli-  
636 gent Robots and Systems (IROS). pp. 7865–7871. IEEE (2021) [4](#)
- 637 46. Rajeswaran, A., Kumar, V., Gupta, A., Vezzani, G., Schulman, J., Todorov, E.,  
638 Levine, S.: Learning complex dexterous manipulation with deep reinforcement  
639 learning and demonstrations. *arXiv preprint arXiv:1709.10087* (2017) [2](#), [4](#)
- 640 47. Rusu, A.A., Colmenarejo, S.G., Gulcehre, C., Desjardins, G., Kirkpatrick, J., Pas-  
641 canu, R., Mnih, V., Kavukcuoglu, K., Hadsell, R.: Policy distillation. *arXiv preprint  
642 arXiv:1511.06295* (2015) [4](#)
- 643 48. Schmeckpeper, K., Rybkin, O., Daniilidis, K., Levine, S., Finn, C.: Reinforce-  
644 ment learning with videos: Combining offline observations with interaction. *arXiv  
645 preprint arXiv:2011.06507* (2020) [4](#)
- 646 49. ShadowRobot: Shadowrobot dexterous hand (2005), <https://www.shadowrobot.com/dexterous-hand-series/> [9](#)
- 647 50. Siahkoohi, A., Louboutin, M., Herrmann, F.J.: Neural network augmented wave-  
648 equation simulation. *arXiv preprint arXiv:1910.00925* (2019) [4](#)
- 649 51. Suh, H., Wang, Y.: Comparing effectiveness of relaxation methods for warm start-  
650 ing trajectory optimization through soft contact (2019) [3](#), [6](#)
- 651 52. Suh, H.J.T., Pang, T., Tedrake, R.: Bundled gradients through contact via random-  
652 ized smoothing. *IEEE Robotics and Automation Letters* **7**(2), 4000–4007 (2022)  
653 [11](#)

- 655 53. Taheri, O., Ghorbani, N., Black, M.J., Tzionas, D.: Grab: A dataset of whole-  
656 body human grasping of objects. In: Computer Vision–ECCV 2020: 16th European  
657 Conference, Glasgow, UK, August 23–28, 2020, Proceedings, Part IV 16. pp. 581–  
658 600. Springer (2020) 10 655
- 659 54. Tan, K.K., Wang, Q.G., Hang, C.C.: Advances in PID control. Springer Science &  
660 Business Media (2012) 12 656
- 661 55. Tedrake, R., the Drake Development Team: Drake: Model-based design and verifi-  
662 cation for robotics (2019), <https://drake.mit.edu> 2 657
- 663 56. Todorov, E., Erez, T., Tassa, Y.: Mujoco: A physics engine for model-based control.  
664 In: 2012 IEEE/RSJ international conference on intelligent robots and systems. pp.  
665 5026–5033. IEEE (2012) 2 658
- 666 57. Traoré, R., Caselles-Dupré, H., Lesort, T., Sun, T., Díaz-Rodríguez, N., Filliat, D.:  
667 Continual reinforcement learning deployed in real-life using policy distillation and  
668 sim2real transfer. arXiv preprint arXiv:1906.04452 (2019) 4 659
- 669 58. Villegas, R., Ceylan, D., Hertzmann, A., Yang, J., Saito, J.: Contact-aware retar-  
670 geting of skinned motion. In: Proceedings of the IEEE/CVF International Confer-  
671 ence on Computer Vision. pp. 9720–9729 (2021) 11 660
- 672 59. Wang, Y., Weidner, N.J., Baxter, M.A., Hwang, Y., Kaufman, D.M., Sueda, S.:  
673 Redmax: Efficient & flexible approach for articulated dynamics. ACM Transactions  
674 on Graphics (TOG) 38(4), 1–10 (2019) 2, 5, 6 661
- 675 60. Wang, Y., Lin, J., Zeng, A., Luo, Z., Zhang, J., Zhang, L.: Physhoi: Physics-based  
676 imitation of dynamic human-object interaction. arXiv preprint arXiv:2312.04393  
677 (2023) 2, 4 662
- 678 61. Watson, L.T., Haftka, R.T.: Modern homotopy methods in optimization. Computer  
679 Methods in Applied Mechanics and Engineering 74(3), 289–305 (1989) 2 663
- 680 62. Wu, Y.H., Wang, J., Wang, X.: Learning generalizable dexterous manipulation  
681 from human grasp affordance. In: Conference on Robot Learning. pp. 618–629.  
682 PMLR (2023) 2, 4 664
- 683 63. Xiong, S., He, X., Tong, Y., Deng, Y., Zhu, B.: Neural vortex method: from finite  
684 lagrangian particles to infinite dimensional eulerian dynamics. Computers & Fluids  
685 258, 105811 (2023) 4 665
- 686 64. Xu, J., Chen, T., Zlokapa, L., Foshey, M., Matusik, W., Sueda, S., Agrawal, P.: An  
687 end-to-end differentiable framework for contact-aware robot design. arXiv preprint  
688 arXiv:2107.07501 (2021) 6, 7 666
- 689 65. Yamane, K., Nakamura, Y.: Stable penalty-based model of frictional contacts. In:  
690 Proceedings 2006 IEEE International Conference on Robotics and Automation,  
691 2006. ICRA 2006. pp. 1904–1909. IEEE (2006) 7 667
- 692 66. Yao, H., Song, Z., Chen, B., Liu, L.: Controlvae: Model-based learning of generative  
693 controllers for physics-based characters. ACM Transactions on Graphics (TOG)  
694 41(6), 1–16 (2022) 2, 9, 11 668
- 695 67. Zeng, A., Song, S., Lee, J., Rodriguez, A., Funkhouser, T.: Tossingbot: Learning  
696 to throw arbitrary objects with residual physics. IEEE Transactions on Robotics  
697 36(4), 1307–1319 (2020) 4 669
- 698 68. Zhang, H., Christen, S., Fan, Z., Zheng, L., Hwangbo, J., Song, J., Hilliges, O.:  
699 Artigrasp: Physically plausible synthesis of bi-manual dexterous grasping and articu-  
700 lation. arXiv preprint arXiv:2309.03891 (2023) 2, 4 670
- 701 69. Zhang, S., Liu, B., Wang, Z., Zhao, T.: Model-based reparameterization policy gra-  
702 dient methods: Theory and practical algorithms. Advances in Neural Information  
703 Processing Systems 36 (2024) 4 671

- 704 70. Zhang, Y., Clegg, A., Ha, S., Turk, G., Ye, Y.: Learning to transfer in-hand manip-  
705 ulations using a greedy shape curriculum. In: Computer Graphics Forum. vol. 42,  
706 pp. 25–36. Wiley Online Library (2023) 4  
707 71. Zhao, W., Queralta, J.P., Westerlund, T.: Sim-to-real transfer in deep reinforce-  
708 ment learning for robotics: a survey. In: 2020 IEEE symposium series on compu-  
709 tational intelligence (SSCI). pp. 737–744. IEEE (2020) 4  
710 72. Zhuang, F., Qi, Z., Duan, K., Xi, D., Zhu, Y., Zhu, H., Xiong, H., He, Q.: A  
711 comprehensive survey on transfer learning. Proceedings of the IEEE 109(1), 43–  
712 76 (2020) 4